Chinese Chemical Letters 32 (2021) 1747–1750

Contents lists available at ScienceDirect

Chinese Chemical Letters

journal homepage: www.elsevier.com/locate/cclet

Communication

Application of adaptive pressure-driven microfluidic chip in thyroid function measurement

Xingshang Xu[a,c], Nongyue He[a,b,*]

[a] State Key Laboratory of Bioelectronics, School of Biological Science and Medical Engineering, Southeast University, Nanjing 210096, China
[b] Hunan Key Laboratory of Biomedical Nanomaterials and Devices, College of Life Sciences and Chemistry, Hunan University of Technology, Zhuzhou 412007, China
[c] Nanjing Lanyu Biotechnology Co., Ltd., Nanjing 210000, China

ARTICLE INFO

Article history:
Received 3 December 2020
Received in revised form 4 January 2021
Accepted 4 January 2021
Available online 9 January 2021

Keywords:
Microfluidic chip
Adaptive pressure drive
Thyroid dysfunction
In vitro diagnosis
Whole blood injection

ABSTRACT

The improvement in accuracy of *in vitro* diagnosis has always been the focus of early screening of thyroid dysfunction. We constructed a microfluidic chip based on a polystyrene polymer substrate. Total triiodothyronine (TT3), total thyroxine (TT4), free triiodothyronine (FT3), free thyroxine (FT4), and thyrotropin (TSH) in human whole blood samples were analysed by fluorescence immunoassay to evaluate thyroid function. The results indicate that the microfluidic chip shows a good linear relationship in the detection of TT3, TT4, FT3, FT4, and TSH standards, and the correlation coefficient (r) is not less than 0.9900. In addition, the chip also has strong anti-interference (RSD% $\leq$ 5%) and good repeatability (CV $\leq$ 8%), and its inter-batch differences are small (CV $\leq$ 15%). The results of practical application in clinical thyroid function measurement indicated its high accuracy ($r \geq 0.9900$). It provides a new method for the determination of thyroid function and lays a foundation for subsequent clinical application.

Thyroid is an important endocrine and metabolic organ responsible for regulating metabolism and life activities in the human body [1–3]. Abnormal functioning of thyroid will lead to hyperthyroidism or hypothyroidism. The hypothyroidism is a long course disease with slow inception, and is difficult to detect in the early clinical stage owing to its significantly lower specificity. This may lead patients to delay the best treatment time. Therefore, early diagnosis and treatment can reduce the adverse effects of thyroid dysfunction [4,5]. In general, the thyroid gland regulates thyroid function by producing follicle-stimulating hormone (FSH) and releasing T3 and T4 in the serum. When T3 and T4 are released in significantly large amount, it will inhibit adenylate cyclase and consequently the level of TSH will be reduced. Therefore, thyroid dysfunction can be diagnosed by detecting the levels of TT3, TT4, FT3, FT4, and TSH [6–9].

At present, various methods including radioimmunoassay (RIA), immunoradiometric (IRMA), and immune-chemiluminescence (ICMA) are used for the detection of thyroid abnormalities [10,11]. Among these, the sensitivity of RIA is lower and it can only detect primary hypothyroidism, but not hyperthyroidism. Therefore, its application is limited [12]. Some advancements were made in the IRMA based on RIA to improve its specificity and sensitivity. Hyperthyroidism can be detected through IRMA but its severity cannot be determined. Moreover, it causes radioactive element pollution similar to RIA [13]. The ICMA turns radioisotopes into chemiluminescent or fluorescent substances on the basis of IRMA, which avoids radioactive contamination and a short use cycle, and also has the advantages of good stability and high sensitivity. However, the above detection methods can be employed in hospital laboratories, and some hospitals with only basic facilities cannot use these techniques. Furthermore, these methods are costly and require longer time for the detection. Consequently, some patients cannot undergo early screening [14–16]. Therefore, it has become the focus of the current research to find a rapid, easy-to-operate, and low-cost diagnosis method.

Microfluidic technology is a technology that can accurately control and manipulate microscale fluids. Because of its various advantages, such as small sample volume and fast reaction speed, microfluidic technology has become an ideal platform for the development of low-cost and high-accuracy disease diagnosis technology [17–21]. At present, the research related to microfluidic control in disease diagnosis mainly focuses on nucleic acid sequencing, biomarker immunoassay, cell recognition, sorting, *etc*. [22,23]. The microfluidic chip can introduce reagents or antibodies sequentially through microchannels, and complete the

* Corresponding author at: State Key Laboratory of Bioelectronics, School of Biological Science and Medical Engineering, Southeast University, Nanjing 210096, China.
E-mail address: nyhe1958@163.com (N. He).

https://doi.org/10.1016/j.cclet.2021.01.008

sample pre-treatment and separation on the chip, which is especially suitable for the detection of trace substances in clinical blood, urine, and other complex samples [24,25]. It has been observed that microfluidic chips can be used in the detection of tumour markers, infectious disease-related viruses, sex hormones or hormone metabolites, cytological diagnosis, and *in vitro* drug metabolism [26–28]. However, the microfluidic chips currently available in the market generally have some defects such as high cost, complex production process, and low rate of good products [29]. The purpose of this study is to develop an adaptive pressure-driven microfluidic chip that can accurately control the flow direction and rate of the liquid in the chip to achieve accurate quantification, and should be compatible with time-resolved fluorescence immunodetection technology for high accuracy and repeatability of detection results. It is applied to the clinical detection of the thyroid function index, which provides a new method for the determination of thyroid function index.

Fluorescent microspheres were purchased from Bangs Laboratories (Indiana, USA); TT3, TT4, and TSH antibodies were acquired from Lanxuan, Suzhou (Jiangsu, China); streptavidin was obtained from Thermo Fisher Scientific (Massachusetts, USA); and Tris-HCl, NaCl, Tween-20, and bovine serum albumin (BSA) solutions were sourced from Sigma Co., Ltd. (Missouri, USA). All reagents were prepared in pure water.

The constant temperature incubator HH·CP-01 was purchased from Shanghai Boxun Medical Biological Instruments Co., Ltd. (Shanghai, China); the centrifuge H1650R was purchased from Hunan Xiangyi Laboratory Instrument Development Co., Ltd. (Hunan, China); the vacuum drying oven DZF-6050AB was sourced from Shanghai Lichen Bangxi instrument Technology Co., Ltd. (Shanghai, China); and HS-AFM ultra-high speed video grade atomic force microscope (AFM) acquired from Research Institute of Biomolecule Metrology Co., Ltd. (Tsukuba, Japan).

The improved polystyrene polymer composite was used as the base and moulded by injection moulding. The entire chip adopts three-layer (upper, middle, and lower) structure, which comprises four main components: microchannel, injection cavity, waste liquid cavity, and quantitative reaction cavity. The lower chip is provided with a microchannel connected to the entire system, and the middle chip is provided with an injection cavity, a waste liquid cavity, and a quantitative reaction cavity (Fig. 1).

The quantitative reaction chamber was irradiated under a UV lamp for 3 min to produce active intermediates such as free radicals. Fluorescent microspheres (4.0 μL) were added to the centre of the chip, and the modified microfluidic chip was drained for 30 min. It was incubated in a coating solution at 37 °C and 80.0% humidity (30 mmol/L Tris-HCl dissolved in 0.50% NaCl, 0.05% Tween-20, and 2.00 μg antibodies) for 1 h. After incubation, it was sealed in a 10.0 mmol/L phosphate-buffered saline containing 1% bovine serum albumin and 0.050% Tween-20 for 30 min, washed with deionised water to remove free antibodies, and drained *in vacuum* to obtain antibody-modified microfluidic chips. The untreated and modified antigen-antibody chips were characterised by AFM.

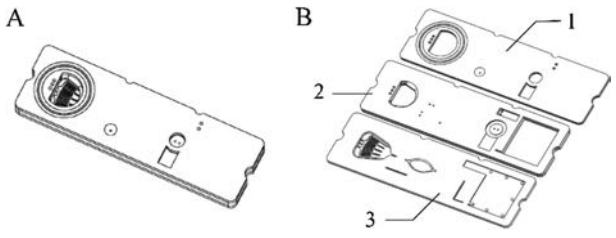

Fig. 1. Schematic diagram of adaptive pressure driven microfluidic chip. (A) The cTnI microfluidic chip panoramic diagram. (B) Three-layer structure diagram of microfluidic chip: 1. Front view of the upper layer of the microfluidic chip; 2. Front view of the middle layer of microfluidic chip; 3. Front view of lower layer of microfluidic chip.

Standard solutions of TT3, TT4, FT3, FT4, and TSH were prepared at different concentrations. The samples of each concentration were tested using a microfluidic chip three times, and the average value of the results was linearly fitted with the theoretical concentration. The background noise value is detected, and the sample signal, which is three times higher than the background signal value, is used as the minimum detection limit for each antibody detected by the microfluidic chip.

The concentrations of TT3, TT4, FT3, FT4, and TSH standard solutions were 0.821 ng/mL, 120.59 ng/mL, 2.00 pg/mL, 9.92 pg/mL, and 1.02 μIU/mL, respectively. The microfluidic chip was used to repeat the measurement 20 times, and the average (X) and standard deviation (SD) of the measured values were calculated. The coefficient of variation (CV) was calculated according to Eq. 1. $CV \leq 8\%$ indicates a good repeatability.

$$CV = SD/X \times 100\% \quad (1)$$

Twenty batches of microfluidic chips were used to detect TT3, TT4, FT3, FT4, and TSH standard solutions with a concentration of 3.243 ng/mL, 30.28 ng/mL, 4.00 pg/mL, 20.08 pg/mL, and 25.35 μIU/mL, respectively. Each test was repeated three times, and X and SD for each concentration were calculated. If the CV obtained from Eq. 1 is less than or equal to 15%, the inter-batch difference is small.

To prevent the content of the components to be tested from being affected by other components, it is necessary to determine its anti-interference. Highly concentrated haemoglobin, bilirubin, and triglycerides were added to the standards with lower concentrations, and the SDs were calculated for three parallel tests.

The venous blood samples of 40 patients were obtained and anticoagulants were added to prevent blood clotting. Because the prepared microfluidic chip can realise the automatic separation of whole blood, it can be detected directly. The detection results were compared with those of the Roche electrochemiluminescence immuno-luminescence instrument commonly used in hospitals, and the correlation of the concentration of the indexes measured by the two methods was observed, and each sample was tested thrice.

The surface of the microfluidic chip was characterised by AFM, and the results are shown in Fig. 2. The root-mean-square roughness (RMS) for untreated chips, the chip modified with

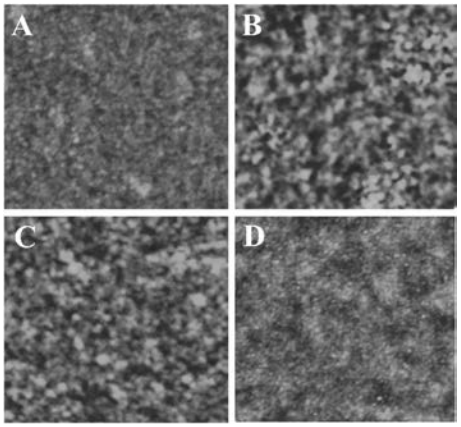

Fig. 2. AFM diagram of microfluidic chip. (A) Untreated chip surface. Modification of TT3 (B), TT4 (C) and TSH (D) antigen and antibody on the surface of the chip.

TT3 antigen, chip modified with TT4 antigen and antibody, and chip modified with TSH antigen and antibody were observed as 4.30, 5.50, 6.20, and 7.10 Å, respectively.

The prepared microfluidic chip was used to detect different concentrations of TT3, TT4, FT3, FT4, and TSH standard solutions. The standard curve is shown in Fig. S1 (Supporting information), and the linear equation is presented in Table 1. By detecting the sample signal, which was three times higher than the background noise, the detection limits of TT3, TT4, FT3, FT4, and TSH were found as 0.195 ng/mL, 1.00 ng/mL, 0.260 pg/mL, 1.00, pg/mL and 0.100 μIU/mL, respectively.

The repeatability and inter-batch difference results of the microfluidic chip are shown in Figs. S2 and S3 (Supporting information), respectively. The CV value of its stability is less than 8%, and that of the inter-batch difference is less than 15%, indicating that the repeatability of the microfluidic chip is significant and the inter-batch difference is small. The results of anti-interference are shown in Table S1 (Supporting information). The results show that under the interference of high concentrations of haemoglobin, bilirubin, and triglycerides, the relative standard deviation (RSD) is less than 5%, indicating that the microfluidic chip has strong anti-interference.

The thyroid function of 40 patients was detected by microfluidic core control and results are compared with those of the Roche electrochemiluminescence immuno-luminescence method commonly used in hospitals. As shown in Fig. 3, the concentrations of five thyroid indexes measured by the microfluidic chip are closely related to the results of the Roche electrochemiluminescence immuno-luminescence method.

The microfluidic chip transfers the function of the analytical laboratory to the microchip to make the analytical device integrated and portable. Because of its advantages of controllable liquid flow, fast reaction, and low sample consumption, it has received significant attention in clinical research and *in vitro* diagnosis [30–33]. Xing *et al*. [34] designed a microfluidic chip for separating and collecting red blood cells and white blood cells in whole blood. After testing, it was found that the removal rate of white blood cells reached 27.4%, and the removal rate of red blood cells was more than 95%. It saves considerable time for follow-up clinical and basic research.

The microfluidic chip designed in this study has various advantages including whole blood injection, accurate quantification, and biosafety, using adaptive pressure to drive blood samples into the channel and passing through multi-layer biofilms to filter impurities such as red blood cells. Moreover, the designed three-dimensional S-shaped channel can ensure the continuous flow of blood samples without air bubbles to ensure that the volume of the samples to be tested does not change, eliminating the work of sample pre-treatment. To prevent the backflow of the sample, we also designed an anti-backflow device to ensure the positive flow

Table 1
Linear relationship between fluorescence intensity and concentration of each standard.

Detection object	Standard curve	Detection range	Detection limit
TT3	$y = -5.0346x + 35.5278$ $R^2 = 0.9995$, $r = -0.9997$	0.195–6.51 ng/mL	0.195 ng/mL
TT4	$y = -0.1660x + 42.5417$ $R^2 = 0.9988$, $r = -0.9994$	1.00–240 ng/mL	1.00 ng/mL
FT3	$y = -3.0775x + 108.3581$ $R^2 = 0.9989$, $r = -0.9995$	0.260–32.55 pg/mL	0.260 pg/mL
FT4	$y = -0.8481x + 87.5107$ $R^2 = 0.9997$, $r = -0.9998$	1.00–100 pg/mL	1.00 pg/mL
TSH	$y = 3.5859x - 2.0077$ $R^2 = 0.9989$, $r = 0.9995$	0.100–100 μIU/mL	0.100 μIU/mL

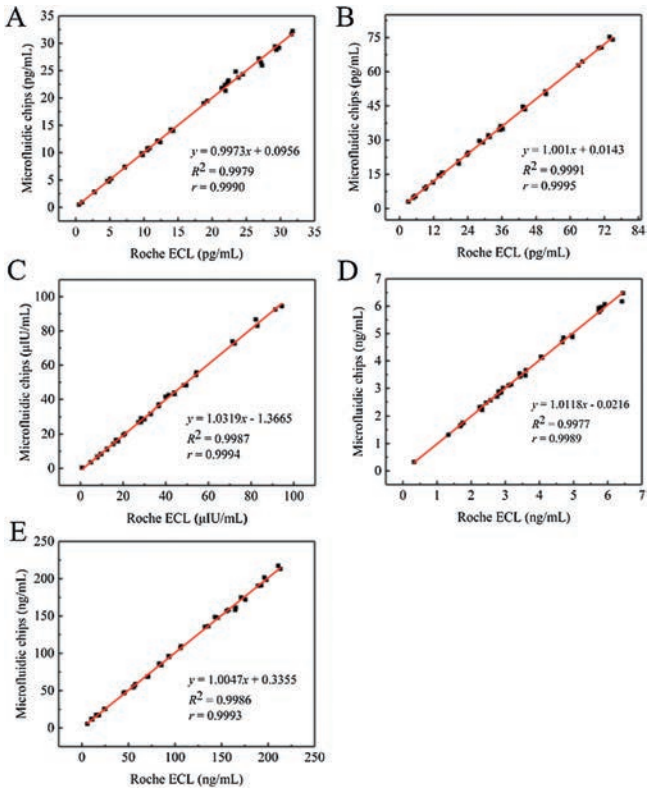

Fig. 3. Comparison of clinical detection results between microfluidic chip detection method and Roche ECL method. (A) TT3; (B) TT4; (C) FT3; (D) FT4; and (E) the TSH.

of the blood sample. The resistance change of the liquid flow is identified by the conductive rubber sensor to accurately control the reaction time, reaction volume, and reaction position of the liquid sample, and achieve accurate quantification. In addition, in this study, a super-large waste tank of 1000 μL was designed to ensure that the reacted samples will not flow out, and biosafety can be ensured as much as possible.

Through the determination of the detection range, anti-interference, repeatability, and inter-batch difference of the chip, it was found that all the indexes of the chip are in line with the standard. Meanwhile, we used the chip in the test of clinical samples, and compared the results with those of the Roche electrochemiluminescence immuno-luminescence method. The results show that the correlation between the two detection methods is good, indicating that it can be used for the clinical detection of thyroid dysfunction. Because of its low production cost, it has laid the foundation for its subsequent marketization and commercialisation.

In this work, an adaptive pressure-driven microfluidic chip was developed that can control the flow direction and rate of liquid in the chip to achieve accurate quantification, and is compatible with time-resolved fluorescence immunodetection technology in order to achieve high accuracy and high repeatability of detection results. The results of its application in the clinical detection of thyroid function are highly correlated with those of the Roche electrochemiluminescence immuno-luminescence instrument commonly used in clinics. This finding provides a new method for the clinical determination of thyroid function.

Declaration of competing interest

The authors report no declarations of interest.

Appendix A. Supplementary data

Supplementary material related to this article can be found, in the online version, at doi:https://doi.org/10.1016/j.cclet.2021.01.008.

References

[1] J. Yang, Nanosci. Nanotechnol. Lett. 12 (2020) 125–131.
[2] Z. Xu, K. Yang, X. Li, Mater. Express 10 (2020) 363–373.
[3] Y. Cao, M. Zheng, W. Cai, Z. Wang, Chin. Chem. Lett. 31 (2020) 463–467.
[4] F. Wu, J. Xu, M. Jin, et al., J. Biomed. Nanotechnol. 16 (2020) 885–898.
[5] H. Wang, W. Ding, L. Peng, et al., J. Biomed. Nanotechnol. 16 (2020) 594–602.
[6] D. Wang, X. Liu, X. Ye, et al., Mater. Express 10 (2020) 934–941.
[7] K. Ren, J. Ma, B. Zhou, et al., Mater. Express 10 (2020) 1189–1196.
[8] Q. Rahman, A. Ali, N. Ahmad, et al., J. Nanosci. Nanotechnol. 20 (2020) 7716–7723.
[9] K. Marbou, W. Gil, A. Ghaferi, et al., J. Nanosci. Nanotechnol. 20 (2020) 7644–7652.
[10] S. Ahmadi, N. Rabiee, Y. Fatahi, et al., J. Biomed. Nanotechnol. 16 (2020) 553–582.
[11] K. Lin, J. Qian, Z. Zhao, G. Wu, H. Wu, J. Nanosci. Nanotechnol. 20 (2020) 7653–7658.
[12] F. Bloise, A. Santos, J. De Brito, et al., Thyroid 30 (2020) 1079–1090.
[13] M. Liu, G. Xu, Z. Huang, et al., Int. J. Artif. Organs 34 (2011) 577–583.
[14] A. Persoon, J. Van Den Ouweland, J. Wilde, et al., Clin. Chem. 52 (2006) 686–691.
[15] G.X. Zhou, Y. Liu, Nanosci. Nanotechnol. Lett. 12 (2020) 245–255.
[16] A. Bolliger, P. Graham, V. Richard, et al., Vet. Clin. Pathol. 31 (2002) 3–8.
[17] H. Chen, Y. Li, Z. Zhang, S. Wang, Biomicrofluidics 14 (2020) 041502.
[18] A. Basiri, A. Heidari, M. Nadi, et al., Rev. Med. Virol. (2020) e2154.
[19] X. Li, S. Hong, C. Tan, et al., Mater. Express 10 (2020) 177–189.
[20] M. Linsenmeier, M. Kopp, S. Stavrakis, A. De Mello, P. Arosio, Biochim. Biophys. Acta: Mol. Cell Res. 1868 (2020) 118823.
[21] Z. Sun, C. Yang, M. Eggersdorfer, et al., Chin. Chem. Lett. 31 (2020) 249–252.
[22] H. Wang, T. Li, Y. Bao, S. Wang, X. Meng, Chin. Chem. Lett. 30 (2019) 403–405.
[23] A. Vasala, V. Hytönen, O. Laitinen, Front. Cell. Infect. Microbiol. 10 (2020) 308.
[24] Z. Wang, L. Cheng, X. Wei, et al., Biomed. Microdevices 22 (2020) 75.
[25] Z. Shi, G. Li, Y. Hu, Chin. Chem. Lett. 30 (2019) 1600–1606.
[26] C. Bai, Nanosci. Nanotechnol. Lett. 12 (2020) 170–177.
[27] B. Song, J. Wang, Z. Yan, et al., Bioengineered 11 (2020) 1137–1145.
[28] X. Fang, J. Rong, Y. Deng, M. Jee, J. Nanosci. Nanotechnol. 20 (2020) 7787–7792.
[29] Y.C. Cui, Y.S. Qiu, Q. Wu, et al., J. Biomed. Nanotechnol. 16 (2020) 910–921.
[30] K. Takeuchi, N. Takama, B. Kim, et al., Biomed. Microdevices 21 (2019) 28.
[31] G. Zheng, L. Lu, Y. Yang, et al., Anal. Chem. 90 (2018) 13280–13289.
[32] M. Mofazzal Jahromi, A. Abdoli, M. Rahmanian, et al., Mol. Neurobiol. 56 (2019) 8489–8512.
[33] P. Paiè, R. Martínez Vázquez, R. Osellame, F. Bragheri, A. Bassi, Cytometry 93 (2018) 987–996.
[34] X. Chen, D. Cui, C. Liu, H. Li, Sens. Actuators B 130 (2008) 216–221.